

EFFECT OF SINTERING TEMPERATURE ON THE PHYSICAL PROPERTIES OF THIN $\text{Ag}_2\text{Cu}_2\text{O}_3$ FILMS PREPARED BY PULSED LASER DEPOSITION

I. S. NAJI*, S. H. ABDULWAHE

*Assistant Professor, Physics Dept., Science College, University of Baghdad
Baghdad, IRAQ*

$\text{Ag}_2\text{Cu}_2\text{O}_3$ powders were formed by solid state reaction at different sintering temperature (200°C, 300°C and 600°C). The influence of sintering and annealing temperatures on the structural, surface morphology, optical and electrical properties of the deposited films was studied. The Ag-Cu-O powder which formed at 200°C had a good structure where tetragonal $\text{Ag}_2\text{Cu}_2\text{O}_3$ phase appear as a fundamental phase, while the other showed mixed $\text{Ag}_2\text{Cu}_2\text{O}_3$ and $\text{Ag}_2\text{Cu}_2\text{O}_4$ phases and many binary phases. The heat treatment at 200°C for films improve the structure. AFM micrographs of Ag-Cu-O films revealed that the big grain size of 125nm with irregular shape obtained at sintering temperature equal to 200°C, while the shape become regular with small grain size at 300 and 600°C. The optical band gap decrease from 1.77eV to 1.45eV when sintering temperature increase to 300°C and reach to 1.90eV at 600°C. Heat treatment decrease the energy band. The electrical conductivity decrease with increment of the sintering temperature for as deposited and annealed films.

(Received March 19, 2017; Accepted May 30, 2017)

Keywords: Ag-Cu-O films, Structure and morphological properties, Optical properties, Sensing behavior

1. Introduction

Silver and copper are situated in the same column of the periodical table and that also found together in alloys and same ternary phases of chalcogenides and tellurides [1]. However, the first oxide containing both elements is $\text{Ag}_2\text{Cu}_2\text{O}_3$ which synthesized and prepared by Gomez-Romero et al. in powder form by using a co precipitation method at low temperature [2]. The structure of this compound can be described considering the substitution of Cu(+1) ions by Ag(+1) ones into the metastable Cu_4O_3 (paramelaconite) structure [3].

This ternary oxide crystallizes in a tetragonal structure and the same space group as Cu_4O_3 with $a=0.58857\text{nm}$ and $c=1.06868\text{nm}$ [4], $\text{Ag}_2\text{Cu}_2\text{O}_3$ seems to exhibit a higher thermal stability than silver oxide which is known to decompose into metallic silver at temperature as low as 250°C [5-7].

After one year Majumdar et al. synthesized silver-copper-oxide composite powders by spray pyrolysis of mixtures of aqueous silver and copper nitrates at 1000°C [8]. While in 2001 Adelsberger et al [9] prepared a single crystals of $\text{Ag}_2\text{Cu}_2\text{O}_3$ by solid state reaction of Ag_2O and CuO in high oxygen pressure. The electronic and magnetic properties of $\text{Ag}_2\text{Cu}_2\text{O}_3$ have been reported in 2002 [10]. Pierson et al [11] in 2007 deposited Ag-Cu-O films on glass substrates for the first time with various Cu/Ag ratios by reactive magnetron co-sputtering of silver and copper targets. In 2009 Tseng et al [12] prepared Ag-doped Cu_2O thin films with various Ag contents by DC-reactive co-sputtering method, and showed that Ag-Cu-O (4% Ag) is the mixed phase of Ag_2O -CuO which is most sensitive to light irradiation useful for optoelectronic related applications. The second ternary silver copper oxide compound ($\text{Ag}_2\text{Cu}_2\text{O}_4$) was synthesized by electrochemical oxidation at room temperature of a slurry of $\text{Ag}_2\text{Cu}_2\text{O}_3$ [13]. It has also been obtained from Ozonization of a suspension of $\text{Ag}_2\text{Cu}_2\text{O}_3$ [14]. The silver copper oxides are p-type

*Corresponding author: moonbb_moonaaa@yahoo.com

Semiconductors with high absorption coefficient of $3 \times 10^5 \text{ cm}^{-1}$ which regarded new type of solar energy material [15].

In this paper, Ag-Cu-O powder was synthesized by solid state reaction and their films were deposited on glass substrates by pulsed laser deposition method. The effect of sintering temperature on the structural, surface morphology, optical and electrical properties of the deposited films was studied.

2. Experimental procedure

Black powder of $\text{Ag}_2\text{Cu}_2\text{O}_3$ was synthesized by solid state reaction of AgO (98 %) and Cu_2O (Fluka AG, Buchs SG, Made in Switzerland, 99%) in a various sintering temperature (200, 300, and 600) °C for two hours. The binary compounds mixed and crushed for an hour then pressed under 5 ton to form a target with a pellet shape with (13mm) diameter and (5mm) thickness. The products were characterized by x-ray diffraction. The Silver-Copper-Oxide thin films were deposited on glass substrates at room temperature by pulsed laser deposition (PLD) method. The thickness of the deposited films were in the range of $(200 \pm 5 \text{ nm})$ and $(100 \pm 5 \text{ nm})$ at (200,300)C and 600C respectively. The focused Nd:YAG SHG Q-switching laser beam with a wavelength 1064 nm (pulse width 10nsec and repetition frequency 6Hz) incident on the target surface with an angle equal to 45° . The deposition was carried out inside a vacuum chamber (10^{-2} mbar). The crystal structure analysis of these films was obtained by using X-ray diffractometer type (D₂ Phaser, Bruker company, Germany) for powder and (Miniflex II Rigaku company, Japan) for thin film was used with CuK_α target of wavelength 0.154nm and $2\theta = 10^\circ - 90^\circ$. Surface morphology measurement was done by using atomic force microscopy (AFM) CSPM-AA 3000 contact mode spectrometer, Angstrom Advanced Inc. Company, USA. The optical transmittance of the films was recorded using UV-VIS. spectrophotometer type (SP8001 Metertech, USA) over the wavelength range (190-1100) nm. Electrical properties were carried out by using Hall effect measurement system (3000 HMS, VER 3.5, supplied with Ecopia company).

Laser interferometer was used to measure the film thickness, which was in the range $(200 \pm 20) \text{ nm}$. The gas sensing properties were performed in the specially designed gas sensor test rig. The test rig was used with stainless steel cylindrical test chamber. The chamber had an inlet for the test gas to flow in and an air admittance valve. The changes in the resistance values of sensor which result from interaction with the target NO_2 gas with concentration 5ppm were recorded using a data acquisition system consisting of multi-meter interfaced with a computer.

3. Results and discussion

The Structure of $\text{Ag}_2\text{Cu}_2\text{O}_3$ powders and films have been characterized using x-ray diffraction (XRD). In general the powders have a polycrystalline structure.

Fig. (1a) shows the x-ray diffraction pattern of $\text{Ag}_2\text{Cu}_2\text{O}_3$ powder which sintered at 200°C (P_1), and it exhibited sharp peaks at 26.865° , 33.170° , 55.195° and 66.00° which correspond to reflections from (112), (004), (215) and (411) planes of tetragonal phase of $\text{Ag}_2\text{Cu}_2\text{O}_3$ with preferential orientation in [004] direction. A diffraction peaks are detected at 38.342° , 52.494° , and 57.735° which represent the reflections from (020)/(111), (020)/(121) and (202)/(312) planes of (cubic Ag_2O and monoclinic CuO), (monoclinic AgO and cubic Cu_2O), (monoclinic AgO monoclinic CuO) respectively. The presence of binary compounds which represented silver oxide and copper oxide at the same position gave an evidence that binary compounds become ternary compounds. A small peaks appeared at 28.204° , 30.586° and 31.161° which correspond to reflections from (112), (200) and (013) planes of tetragonal Cu_4O_3 compound. Indeed, these peaks does not match with diffraction peak of Cu_2O and CuO , confirming the synthesis of paramelaconite and the structure is similar of ternary compound $\text{Ag}_2\text{Cu}_2\text{O}_3$.

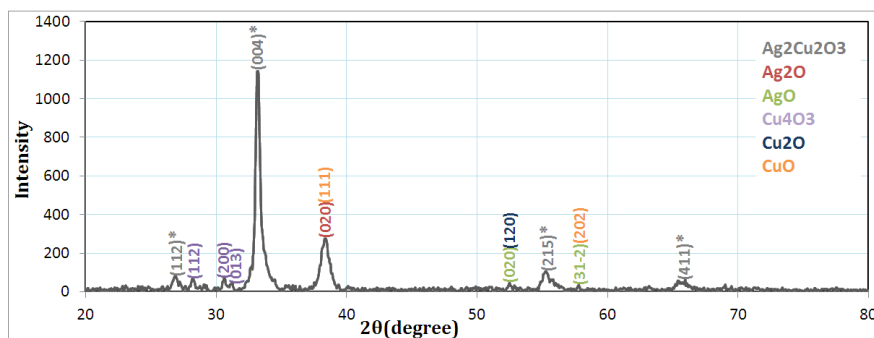


Fig. 1a. X-Ray diffraction pattern of $\text{Ag}_2\text{Cu}_2\text{O}_3$ powder at sintering temperature $200\text{ }^\circ\text{C}$

Table 1a. Structural parameters viz. inter-planar spacing, crystallite size and miller indices of $\text{Ag}_2\text{Cu}_2\text{O}_3$ powder at sintering temperature $200\text{ }^\circ\text{C}$

Sample	2θ (Deg.)	d_{hkl} Exp.(Å)	d_{hkl} Std.	hkl	FWHM (Deg.)	G.S (nm)	phase	card No.
$\text{Ag}_2\text{Cu}_2\text{O}_3$	26.865	3.31596	3.2839	112	0.4166	19.6	tetragonal	96-431-9055
	33.170	2.69866	2.6723	004	0.3333	24.9		
	55.195	1.66279	1.6595	215	0.5	17.9		
	66	1.4143	1.4150	411	1.25	7.6		
Ag_2O	38.342	2.34567	2.3590	020	0.6944	12.1	Cubic	96-101-0487
AgO	52.494	1.74182	1.7390	020	0.2777	31.9	monoclinic	96-900-8963
	57.735	1.59553	1.5934	31 $\bar{2}$	0.2222	40.8		
Cu_4O_3	28.204	3.16153	3.1742	112	0.2777	29.5	tetragonal	96-900-0604
	30.586	2.92055	2.9185	200	0.1944	42.4		
	31.161	2.86796	2.8797	013	0.2777	29.7		
Cu_2O	52.494	1.74182	1.7431	121	0.2777	31.9	Cubic	96-900-5770
CuO	38.342	2.34567	2.3395	111	0.6944	12.1	monoclinic	96-410-5683
	57.735	1.59553	1.5963	202	0.2222	40.8		

The XRD pattern for $\text{Ag}_2\text{Cu}_2\text{O}_3$ powder which sintered at 300°C (P_2) is shown in fig. (1b). It is clear that the intensity of the fundamental peak of $\text{Ag}_2\text{Cu}_2\text{O}_3$ phase which correspond the reflection from (004) plane decrease and appear a new peak at 34.973° for (211) plane. The spectrum contained (200), (004), (211), (215), (224), (323), (035), (411) and (332) planes for $\text{Ag}_2\text{Cu}_2\text{O}_3$ phase. XRD was detected in addition to $\text{Ag}_2\text{Cu}_2\text{O}_3$ another oxide phase such as $\text{Ag}_2\text{Cu}_2\text{O}_4$ at 57.376° for (-113) plane which represent second ternary silver copper oxide compound. Also there is a binary compounds such as AgO, Ag_2O , CuO, Cu_2O and Cu_4O_3 . There is a two high intensity peaks appeared at 32.930° and 38.205° which represent the same position of (cubic Ag_2O / monoclinic CuO). These two diffraction peaks may attributed to silver-copper oxide solid solutions. The diffraction peaks with (112), (413) and (316) planes which related to tetragonal Cu_4O_3 were appeared. A two peaks at 37.759° and 44.385° which related to the diffraction from (111) and (200) plans of Ag are appeared. This is math with Hari Prasad Reddy et al. [6], Narayana Reddy et al. [16]. The presence of Ag element attributed to the lower reactivity of silver atoms versus oxygen compared with that of copper ones. This is not surprising because silver oxide that is known to decompose into metallic silver at temperature as low as 250°C [7].

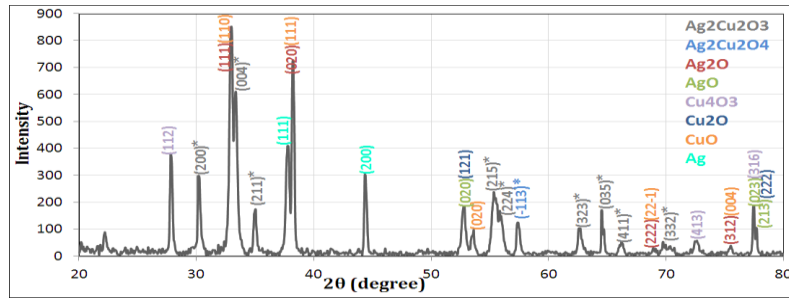


Fig.1b. X-Ray diffraction pattern of $\text{Ag}_2\text{Cu}_2\text{O}_3$ powder at sintering temperature 300°C

Table 1b. Structural parameters viz. inter-planar spacing, crystallite size and miller indices of $\text{Ag}_2\text{Cu}_2\text{O}_3$ powder at sintering temperature 300°C

Sample	2θ (Deg.)	d_{hkl} Exp.(Å)	d_{hkl} Std.	hkl	FWHM (Deg.)	G.S (nm)	phase	card No.
$\text{Ag}_2\text{Cu}_2\text{O}_3$	30.175	2.95937	2.9431	200	0.2890	28.5	tetragonal	96-431-9055
	33.289	2.68925	2.6723	004	0.2890	28.7		
	34.973	2.56353	2.5560	211	0.2890	28.8		
	55.328	1.65910	1.6595	215	0.5780	15.5		
	55.812	1.64587	1.6419	224	0.4335	20.7		
	62.620	1.48229	1.4842	323	0.2890	32.2		
	64.512	1.44331	1.4455	035	0.1445	65.0		
	66.167	1.41116	1.4150	411	0.4335	21.9		
70.1	1.3413	1.3429	332	1.1560	8.4			
$\text{Ag}_2\text{Cu}_2\text{O}_4$	57.376	1.60466	1.6040	-113	0.2890	31.3	-----	-----
Ag_2O	32.930	2.71780	2.7239	111	0.2890	28.7	Cubic	96-101-0487
	38.205	2.35381	2.3590	020	0.2601	32.3		
	68.98	1.3603	1.3620	222	0.2890	33.4		
	75.431	1.25919	1.2609	312	0.2890	34.7		
AgO	52.730	1.73456	1.7390	020	0.2601	34.1	monoclinic	96-900-8963
	77.436	1.23152	1.2324	023	0.1445	70.5		
	77.66	1.2285	1.2289	213	0.5479	18.6		
Cu_4O_3	27.824	3.20380	3.1742	112	0.6164	13.3	tetragonal	96-900-0604
	72.505	1.30262	1.3017	413	0.3757	26.2		
	77.436	1.23152	1.2324	316	0.1445	70.5		
Cu_2O	52.730	1.73456	1.7383	121	0.2601	34.1	Cubic	96-101-0964
	77.66	1.2285	1.2292	222	0.5479	18.6		
CuO	32.930	2.71780	2.7460	110	0.2890	28.7	monoclinic	96-410-5686
	38.205	2.35381	2.3395	111	0.2601	32.3		96-410-5683
	53.512	1.71105	1.7088	020	0.2890	30.8		96-410-5686
Ag	37.759	2.38055	2.3821	111	0.3468	24.2	Cubic	96-901-3049
	44.385	2.03935	2.0386	200	0.2312	37.1		96-901-2962

Fig. (1C) represent the x-ray diffraction pattern for $\text{Ag}_2\text{Cu}_2\text{O}_3$ powder treated at sintering temperature equal to 600°C (P_3). The pattern can be divided into three domains (ternary compound ($\text{Ag}_2\text{Cu}_2\text{O}_3$), binary compound (silver oxide and copper oxide), and elements (silver and copper). Generally the intensity of $\text{Ag}_2\text{Cu}_2\text{O}_3$ peak is less than the former powders (200, and 300°C) and the base peak appeared at 29.28° reflected from (013) plane for tetragonal structure.

The larger peak represent the position of two binary compounds cubic Ag_2O and monoclinic CuO at reflection surfaces (020) and (111) respectively, and probably these binary compounds become ternary compounds at different ratios when their presence at the same peak. The presence of Ag and Cu elements is due to decompose the ternary and binary compounds at 600°C , this means the ratio of oxygen become un sufficient and there is no pumping O_2 gas during sintering operation. Table (1a, b, and c) illustrate the structural parameters for all compounds.

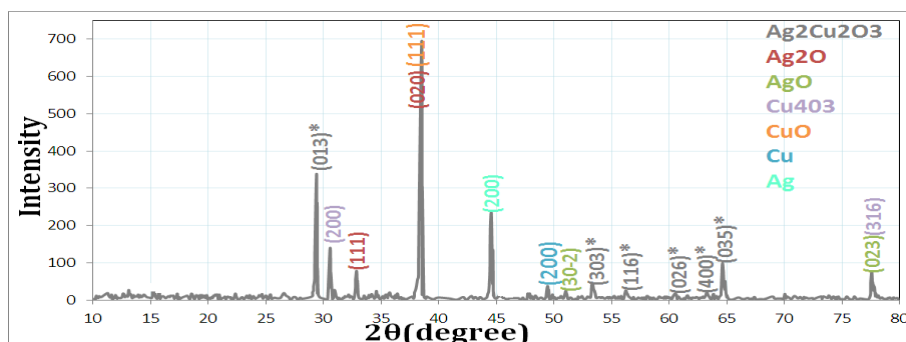


Fig.1c. X-Ray diffraction pattern of $\text{Ag}_2\text{Cu}_2\text{O}_3$ powder at sintering temperature 600°C

Table 1c. Structural parameters viz. inter-planar spacing, crystallite size and miller indices of $\text{Ag}_2\text{Cu}_2\text{O}_3$ powder at sintering temperature 600°C

Sample	2θ (Deg.)	d_{hkl} Exp.(Å)	d_{hkl} Std.	hkl	FWHM (Deg.)	G.S (nm)	phase	card No.
$\text{Ag}_2\text{Cu}_2\text{O}_3$	29.2820	3.0475	3.0481	013	0.2667	30.8	tetragonal	96-431-9055
	53.3150	1.7169	1.7187	303	0.4	22.2		
	56.2190	1.6349	1.6378	116	0.5	18		
	60.5000	1.5291	1.5241	026	0.6667	13.8		
	63.2340	1.4694	1.4715	400	0.3333	28		
	64.6240	1.4411	1.4455	035	0.3	31.3		
Ag_2O	32.8160	2.7270	2.7239	111	0.16666	49.7	Cubic	96-101-0487
	38.312	2.34784	2.3590	020	0.13333	63.1		
AgO	51	1.7893	1.7926	30-2	0.3333	26.4	monoclinic	96-900-8963
	77.5	1.2307	1.2324	023	0.43333	23.5		
Cu_4O_3	30.519	2.92675	2.9185	200	0.1	82.3	tetragonal	96-900-0604
	77.5	1.2307	1.2324	316	0.43333	23.5		
CuO	38.312	2.34784	2.3395	111	0.13333	63.1	monoclinic	96-410-5683
Cu	49.4340	1.8422	1.8460	200	0.26666	32.8	Cubic	96-901-3024
Ag	44.497	2.03448	2.0389	200	0.16666	51.5	Cubic	96-901-2432

The XRD pattern for as deposited $\text{Ag}_2\text{Cu}_2\text{O}_3$ thin films and annealed at 200°C for half an hour for (P1) are shown in Fig. (2). The films have polycrystalline nature. It is obvious that the peaks are sharp which means the crystallinity of the films are good. There is also a shift to higher 2θ with annealing at 200°C , which means the deficiency of O_2 in the films make the lattice constant smaller. Two peaks for as deposited film $\text{Ag}_2\text{Cu}_2\text{O}_3$ appeared at 43.4° and 81.5° for (220) and (424) planes for tetragonal structure of $\text{Ag}_2\text{Cu}_2\text{O}_3$ phase. In addition to the $\text{Ag}_2\text{Cu}_2\text{O}_3$ phase, the XRD analysis of the as deposited film shows the presence of high intensity peak at 37.15° which corresponding the reflections from (111) plane of cubic Cu_2O phase and monoclinic AgO phase. Two small peaks at 64.22° , and 77.32° for tetragonal Cu_4O_3 and monoclinic AgO compounds were observed. The heat treatment for film at 200°C induces modifications of x-ray

diffraction pattern. The ternary compound at 43.4° decompose to binary compound tetragonal Cu_4O_3 (213) and cubic Ag (200). This result agreement with Petitjean et al [7]. Also Cubic Ag_2O phase and monoclinic CuO phase appeared at the same position at 38.14° as a high intensity peak.

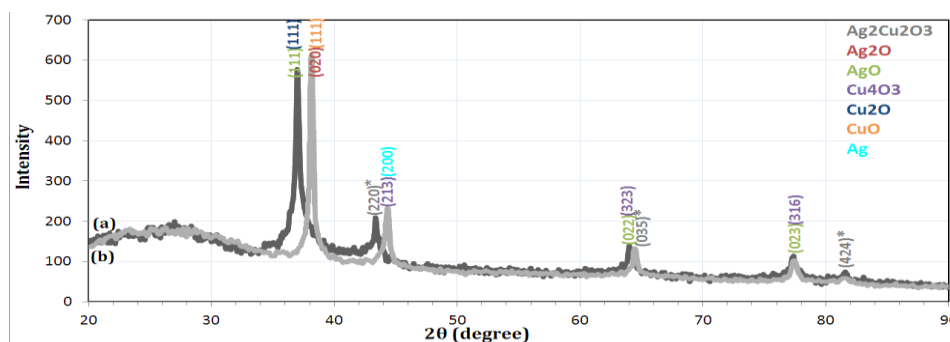


Fig.2. X-Ray diffraction pattern of $\text{Ag}_2\text{Cu}_2\text{O}_3$ Film sintering temperature 200°C (a) as deposited at room temperature (b) annealing at 200°C for half an hour

Table 2a. Structural parameters viz. inter-planar spacing, crystallite size and miller indices of $\text{Ag}_2\text{Cu}_2\text{O}_3$ films at sintering temperature 200°C

Sample	2θ (Deg.)	d_{hkl} Exp.(Å)	d_{hkl} Std.	hkl	FWHM (Deg.)	G.S (nm)	phase	card No.
$\text{Ag}_2\text{Cu}_2\text{O}_3$	43.4	2.0833	2.0811	220	0.612	14.0	tetragonal	96-431-9055
	81.5	1.1801	1.1807	424	0.5369	19.5		
AgO	37.15	2.4182	2.4130	111	0.612	13.7	monoclinic	96-900-8963
	64.22	1.4492	1.4489	022	0.612	15.3		
	77.32	1.2331	1.2324	023	0.635	16		
Cu_4O_3	64.22	1.4492	1.4543	323	0.612	15.3	tetragonal	96-900-0604
	77.32	1.2331	1.2324	316	0.635	16		
Cu_2O	37.15	2.4182	2.4584	111	0.612	13.7	Cubic	96-101-0964

Table 2b. Structural parameters viz. inter-planar spacing, crystallite size and miller indices of $\text{Ag}_2\text{Cu}_2\text{O}_3$ films annealing at 200°C when sintering temperature 200°C

Sample	2θ (Deg.)	d_{hkl} Exp.(Å)	d_{hkl} Std.	hkl	FWHM (Deg.)	G.S (nm)	phase	card No.
$\text{Ag}_2\text{Cu}_2\text{O}_3$	64.5	1.4435	1.4455	035	0.588	16.0	tetragonal	96-431-9055
	81.5	1.1801	1.1807	424	0.857	12.2		
Ag_2O	38.14	2.3576	2.3590	020	0.588	14.3	Cubic	96-101-0487
AgO	77.39	1.2321	1.2324	023	0.706	14.4	monoclinic	96-900-8963
Cu_4O_3	44.3	2.0430	2.0498	213	0.612	14.0	tetragonal	96-900-0604
	77.39	1.2321	1.2324	316	0.706	14.4		
CuO	38.14	2.3576	2.3395	111	0.588	14.3	monoclinic	96-410-5683
Ag	44.3	2.0430	2.0430	200	0.612	14.0	Cubic	96-901-3046

Fig. (3) shows the x-ray diffraction pattern of as deposited and annealed at 200°C $\text{Ag}_2\text{Cu}_2\text{O}_3$ films for (P2), generally the films have polycrystalline structure.

The peaks which appeared in this pattern are not sharp and have low intensity, and very broad diffraction peak appeared in the rang of $2\theta=10^\circ-35^\circ$. It revealed $\text{Ag}_2\text{Cu}_2\text{O}_4$ phase as a fundamental peak at 37.28° which correspond to reflection from (-202) plane for films deposited at room temperature and annealed. Also two peaks detected at 27.01° and 43.50° for tetragonal $\text{Ag}_2\text{Cu}_2\text{O}_3$ phase. A small peaks represent binary compounds are detected at 64.67° and 77.46° which represent the reflections from (022)/(323) and (023)/(316) for monoclinic AgO and tetragonal Cu_4O_3 compounds. When the films annealed at 200°C the peaks becomes more sharp as shown in the figure and tables.

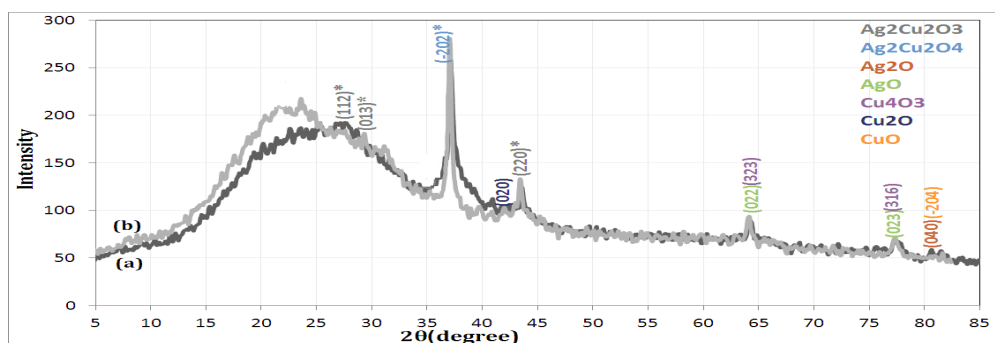


Fig.3. X-Ray diffraction pattern of $\text{Ag}_2\text{Cu}_2\text{O}_3$ Film sintering temperature 300 °C (a) as deposited at room temperature (b) annealing at 200°C for half an hour

Table 3a. Structural parameters viz. inter-planar spacing , crystallite size and miller indices of $\text{Ag}_2\text{Cu}_2\text{O}_3$ films at sintering temperature 300°C

Sample	2θ (Deg.)	d_{hkl} Exp.(Å)	d_{hkl} Std.	hkl	FWHM (Deg.)	G.S (nm)	phase	card No.
$\text{Ag}_2\text{Cu}_2\text{O}_3$	27.01	3.2985	3.2839	112	0.659	12.4	tetragonal	96-431-9055
	43.50	2.0788	2.0811	220	0.565	15.1		
$\text{Ag}_2\text{Cu}_2\text{O}_4$	37.28	2.4100	2.4125	-202	0.612	13.7	-----	-----
Ag_2O	80.63	1.1906	1.1900	040	0.4474	23.3	Cubic	96-101-0605
AgO	64.67	1.4401	1.4489	022	0.671	14.0	monoclinic	96-900-8963
	77.46	1.2312	1.2324	023	0.8948	11.4		
Cu_4O_3	64.67	1.4401	1.4543	323	0.671	14.0	tetragonal	96-900-0604
	77.46	1.2312	1.2324	316	0.8948	11.4		
CuO	80.63	1.1906	1.1933	-204	0.4474	23.3	monoclinic	96-101-1195

Table (3 b) Structural parameters viz. inter-planar spacing , crystallite size and miller indices of $Ag_2Cu_2O_3$ films annealing at $200^\circ C$ when sintering temperature $300^\circ C$

Sample	2 θ (Deg.)	d_{hkl} Exp.(Å)	d_{hkl} Std.	hkl	FWHM (Deg.)	G.S (nm)	phase	card No.
$Ag_2Cu_2O_3$	27.52	3.2385	3.2839	112	0.612	13.4	tetragonal	96-431-9055
	29.33	3.0427	3.0481	013	0.635	12.9		
	43.44	2.0815	2.0811	220	0.565	15.1		
$Ag_2Cu_2O_4$	37.11	2.4207	2.4125	-202	0.588	14.3	-----	-----
Ag_2O	64.35	1.4466	1.4489	022	0.635	14.8	monoclinic	96-900-8963
	77.28	1.2336	1.2324	023	0.75	13.6		
Cu_4O_3	64.35	1.4466	1.4543	323	0.635	14.8	tetragonal	96-900-0604
	77.28	1.2336	1.2324	316	0.75	13.6		
Cu_2O	42	2.1495	2.1348	020	0.682	12.5	Cubic	96-900-5770

The x-ray diffraction pattern of as deposited and annealed at $200^\circ C$ $Ag_2Cu_2O_3$ films for (P3) are shown in Fig. (4). The as deposited $Ag_2Cu_2O_3$ film has an amorphous structure, and the structure improve with annealing, where a weak diffraction peak appeared which related totternary compound at 37.11 for $Ag_2Cu_2O_4$ phase and two peaks at 17.13° and 42.63° correspond to the diffractions from (101)and (213) planes of tetragonal $Ag_2Cu_2O_3$ phase. This result agree with Sreedhar et al.[1] who found that the film deposited at 303K was amorphous. Also a binary compound such as (Ag_2O and CuO) and (Cu_4O_3 and Ag) are detected at same position.

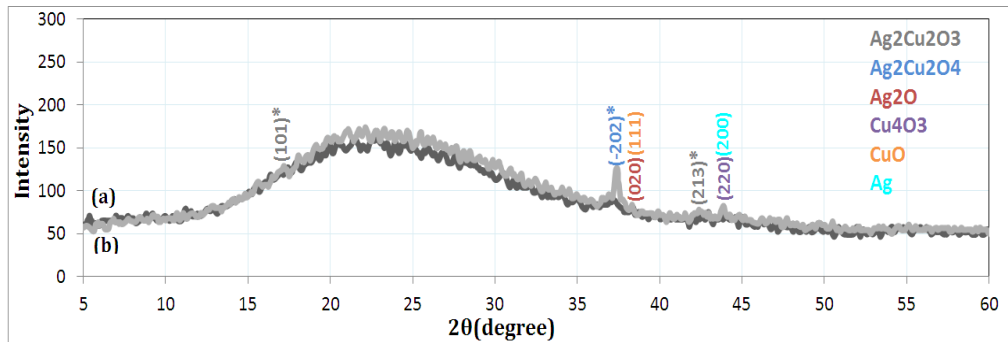


Fig.4. X-Ray diffraction pattern of $Ag_2Cu_2O_3$ Film sintering temperature $600^\circ C$ (a) as deposited at room temperature (b) annealing at $200^\circ C$ for half an hour

Table 4. Structural parameters viz. inter-planar spacing, crystallite size and miller indices of $Ag_2Cu_2O_3$ films annealing at $200^\circ C$ when sintering temperature $600^\circ C$

Sample	2 θ (Deg.)	d_{hkl} Exp.(Å)	d_{hkl} Std.	hkl	FWHM (Deg.)	G.S (nm)	phase	card No.
$Ag_2Cu_2O_3$	17.13	5.1722	5.1561	101	0.8	10.0	tetragonal	96-431-9055
	42.63	2.1191	2.1172	213	0.847	10.1		
$Ag_2Cu_2O_4$	37.35	2.4057	2.4125	-202	0.535	15.7	-----	-----
Ag_2O	38.29	2.3494	2.3590	020	0.5	16.8	Cubic	96-101-0487
Cu_4O_3	43.71	2.0693	2.0637	220	0.753	11.4	tetragonal	96-900-0604
CuO	38.29	2.3494	2.3395	111	0.5	16.8	monoclinic	96-410-5683
Ag	43.71	2.0693	2.0675	200	0.753	11.4	Cubic	96-901-3050

Atomic Force Microscope analysis

It is well known that AFM is one of the most effective ways for the surface analysis due to its high resolution and powerful analysis.

Fig. (5) shows the three dimensional AFM images and histograms of $\text{Ag}_2\text{Cu}_2\text{O}_3$ thin films prepared by Pulsed Laser deposition for different sintering temperature (200, 300 and 600) °C . The deposited film using powder sintered at 200°C (Fig.5a) showed irregular shape of grains with large grain size of 125.53 nm and the root mean square roughness of 0.446 nm. It is also seen that the films has less uniform distribution, and this is may be due to the presence a good ratio of oxygen. The films which formed at 300°C and 600°C (fig. 5b, and c) showed regular shape of grains size equal to 87.87 and 92.79 nm uniform distribution with continuous granular morphology and with a large root mean square roughness of 2.02 and 1.45nm respectively. This result agreement with Reddy et.al. how found the grain size increased to 132nm with the increase of oxygen partial pressure [16]. Table (5) illustrated all parameter which obtained from surface morphology study.

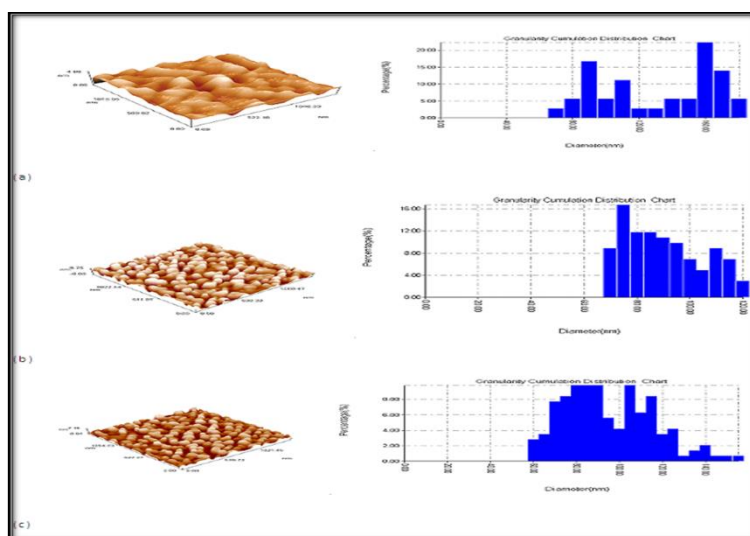


Fig. 5. AFM picture and histogram for as deposited $\text{Ag}_2\text{Cu}_2\text{O}_3$ films when different sintering temperature (a) 200 °C (b) 300 °C and (c) 600 °

Table 5. Average grain size, average roughness, and root mean square for Ag-Cu-O films with different sintering temperature (200 °C, 300 °C and 600 °C)

Thin films	Sintering Temp.	Root mean square (nm)	Grain size (nm)	Roughness average (nm)
$\text{Ag}_2\text{Cu}_2\text{O}_3$	200°C	0.446	125.53	0.342
	300°C	2.02	87.87	1.74
	600°C	1.45	92.79	1.26

The surface morphological results of prepared powder (P1) were studied by SEM images. Fig. (6) shows the microstructure with different magnification (505x, 6013x, 21471x) of $\text{Ag}_2\text{Cu}_2\text{O}_3$ powder which sintered at 200°C as observed by SEM analysis. It is obvious there is agglomerates of oxide particles with platelets shape. There is disorder structure, and this disorder imply either a static disorder for silver positions or a dynamic one, as in ionic conductors. This result also was found by Rojas et al. [17].

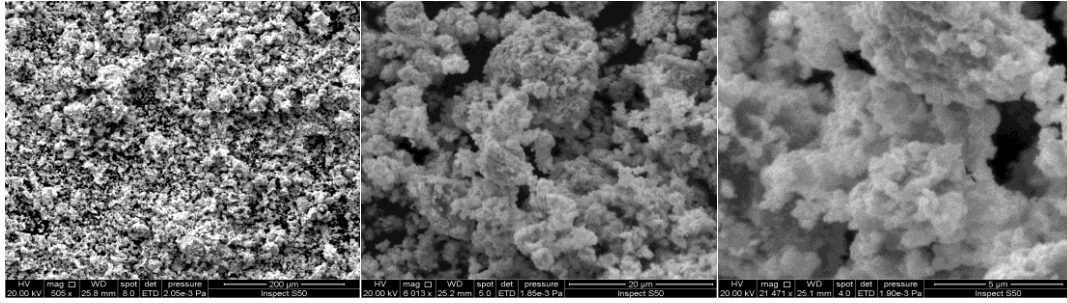


Fig. 6. SEM photograph of $\text{Ag}_2\text{Cu}_2\text{O}_3$ which formed at 200°C

The optical transmittance spectra of the $\text{Ag}_2\text{Cu}_2\text{O}_3$ films formed at sintering temperatures ($200, 300, 600$) $^\circ\text{C}$ which deposited at room temperature and annealed at 200°C for half an hour are shown in Fig (7a & b) respectively.

The deposited films using powder (P_1 & P_2) which sintered at 200°C and 300°C exhibited low optical transmittance of 52.8 % and 53 % at wavelength of 1000nm. The optical transmittance of the film increased and reached to 85.6% with increasing sintering temperature to 600°C .

The low optical transmittance at low sintering temperature was due the scattering of light by the metallic silver atoms present along with $\text{Ag}_2\text{Cu}_2\text{O}_3$ [3]. While the high transmittance at high sintering temperature (600°C) was due to the amorphous structure of these films as shown in X-ray data. It is clear that the optical transmittance of the films critically depends on the sintering temperature.

The films which was annealed at 200°C have the same behavior with little decrease of transparence for all samples, this may attributed to improve the structure with heat treatment.

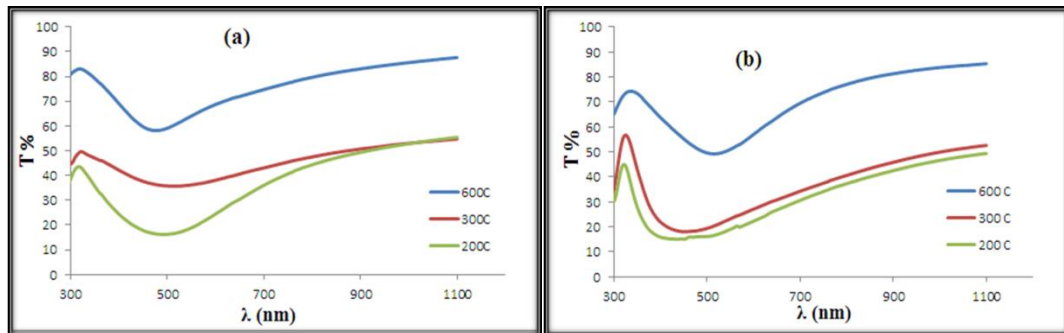


Fig. 7. Optical transmittance versus wavelength of $\text{Ag}_2\text{Cu}_2\text{O}_3$ thin films at different sintering temperature (a) as deposited (b) annealed at 200°C

The optical absorption coefficient (α) was calculated from the optical transmittance (T) data using the relation:

$$\alpha = (1/t) \ln T \quad (1)$$

where it is the film thickness. Fig. (8a&b) show the optical absorption coefficient (α) varies with different preparation or sintering temperature ($200, 300,$ and 600°C) as function of wavelength for as deposited and annealed $\text{Ag}_2\text{Cu}_2\text{O}_3$. The optical absorption coefficient increase gradually at wavelength 300 nm and reach up to the highest peak absorption at wave length range of (390-600) nm and then gradually decreases and reaches to less absorption at a wavelength of 1100nm.

The optical absorption edge of the films as deposited at R.T shifted towards higher wavelength side with increasing sintering temperature to 300°C and then shifted to lower wavelength (blue region) when the sample sintered at 600°C , on the other hand the absorption

edge of annealed films shifted towards lower wavelength and the α increase of become more gradually (not sharp) with increasing sintering temperature.

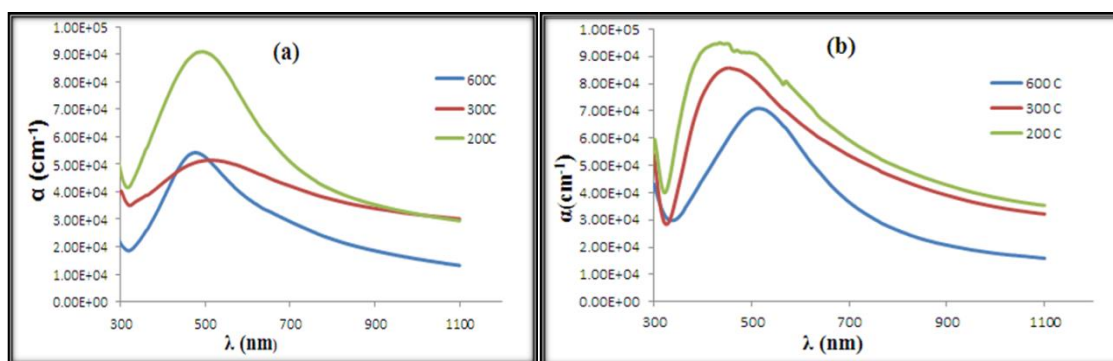


Fig. 8. Absorption coefficient versus wavelength of $\text{Ag}_2\text{Cu}_2\text{O}_3$ thin films at different sintering temperature (a) as deposited (b) annealed at 200°C

The optical band gap (E_g) of $\text{Ag}_2\text{Cu}_2\text{O}_3$ films has been determined from the optical absorption coefficient and photon energy ($h\nu$) data assuming the direct transmission occurs between valance and conduction band using Tauc's relation.

$$\alpha h\nu = B (h\nu - E_g)^{1/2} \quad (2)$$

Where B is a constant inversely proportional to amorphousity. Extrapolation of the linear portion of the plots of $(\alpha h\nu)^2$ versus photon energy to $\alpha = 0$ yields the optical band gap of the $\text{Ag}_2\text{Cu}_2\text{O}_3$ films. Fig. (9a&b) show the plot of $(\alpha h\nu)^2$ versus photon energy ($h\nu$) of as deposited and annealed $\text{Ag}_2\text{Cu}_2\text{O}_3$ films formed at different sintering temperature respectively.

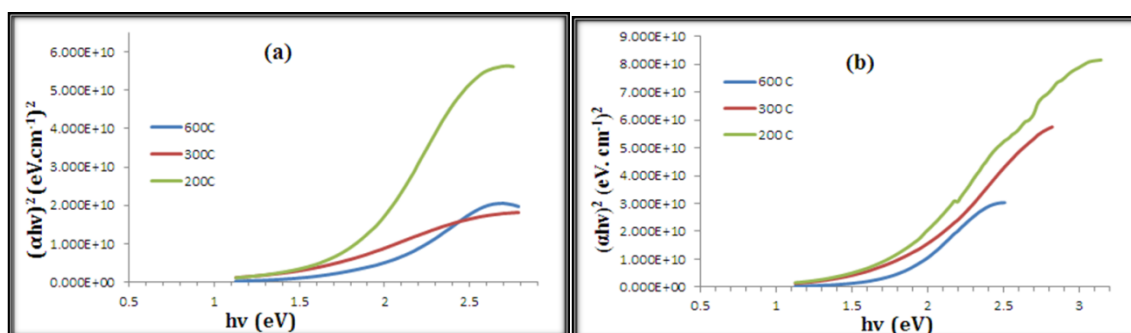


Fig.9. The variation of $(\alpha h\nu)^2$ versus the photon energy ($h\nu$) of $\text{Ag}_2\text{Cu}_2\text{O}_3$ thin films at different sintering temperature (a) as deposited (b) annealed at 200°C

The optical band gap of as deposited films decrease from 1.77 to 1.45 eV with increasing sintering temperature from 200 to 300 $^\circ\text{C}$, and increase to 1.9 eV at 600 $^\circ\text{C}$. The low value of optical band gap at sintering temperature equal to 300 $^\circ\text{C}$ related to appear the $\text{Ag}_2\text{Cu}_2\text{O}_4$ phase as a fundamental phase which have optimum energy gap and better than $\text{Ag}_2\text{Cu}_2\text{O}_3$ phase. The energy gap broadening with increasing sintering temperature to 600 $^\circ\text{C}$, may be related to existence high density of levels within the band gap of energies near the bands.

It is clear from Fig. (9b) that the energy gap decrease when the films annealed at 200 $^\circ\text{C}$. this attributed to improve the structure with annealing.

Fig. (10 a&b) show the variation of refractive index(n) with wavelength(λ) of as deposited and annealed $\text{Ag}_2\text{Cu}_2\text{O}_3$ thin films at different sintering temperature(200,300, 600) $^\circ\text{C}$ respectively. In general it clear that the refractive index decreases with increasing the sintering temperature.

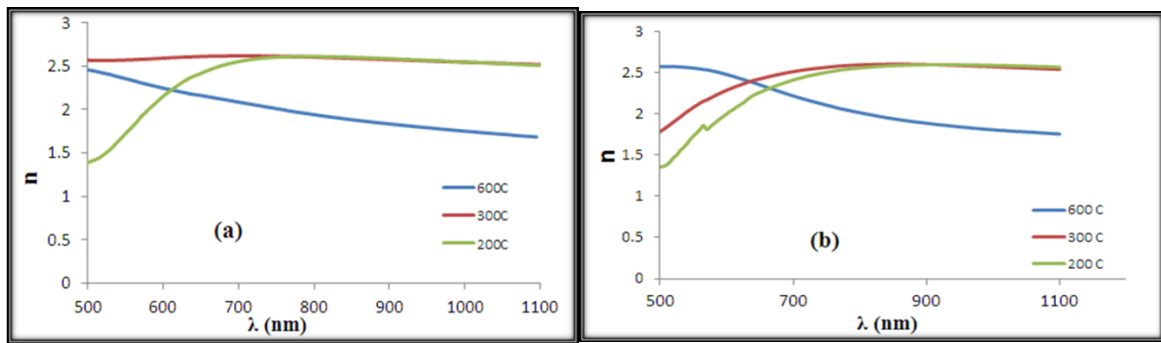


Fig. 10. the variation of refractive Index (n) with wavelength (λ) of $\text{Ag}_2\text{Cu}_2\text{O}_3$ thin films at different sintering temperature (a) as deposited (b) annealed at 200°C

Fig. (11 a&b) shows the variation of extinction coefficient (k) with wavelength (λ) of as deposited and annealed $\text{Ag}_2\text{Cu}_2\text{O}_3$ thin films at different sintering temperature (200, 300, 600) $^\circ\text{C}$ respectively. It is obvious that the extinction coefficient takes the similar behavior of the corresponding absorption coefficient. The decreasing of sintering temperature lead to increase the extinction coefficient (k) and films its shifted towards for annealed higher wavelength side.

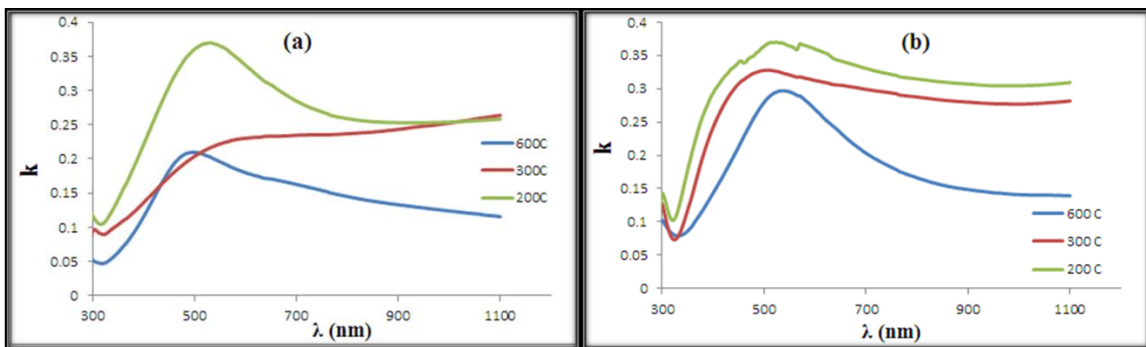


Fig. 11. the variation of extinction coefficient (k) with wavelength (λ) of $\text{Ag}_2\text{Cu}_2\text{O}_3$ thin films at different sintering temperature (a) as deposited (b) annealed at 200°C

The complex dielectric constant is a fundamental material property, the real part of it is associated with term of how much it will slow down the speed of light in the material and the imaginary part gives that how a dielectric absorb energy from electric field due to polarization in it. The behavior of ϵ_r , similar to refractive index because the smaller value of k^2 comparison of n^2 , while ϵ_i is mainly depends on the k values, which are related to the variation of absorption coefficient.

The optical properties parameters including , energy gap, absorption coefficient, refractive index, extinction coefficient, real and imaginary part of the dielectric constant at wavelength equals to 1000nm for as deposited and annealed $\text{Ag}_2\text{Cu}_2\text{O}_3$ films are listed in Table (6).

Table 6. The optical properties for Ag-Cu-O thin film at wavelength equal to 1000nm

Thin film	Sintering Temp.(°C)	E_g (eV)	$\alpha \times 10^4$ (cm) ⁻¹	n	k	ϵ_r	$i\epsilon$
As deposited	200	1.77	3.19	2.548	0.253	6.431	1.294
	300	1.45	3.17	2.546	0.252	6.421	1.286
	600	1.90	1.56	1.750	0.123	3.054	0.434
annealed	200	1.60	3.82	2.590	0.304	6.635	1.578
	300	1.70	3.48	2.576	0.276	6.563	1.426
	600	1.75	1.77	1.810	0.141	3.256	0.510

The type, concentration (n) and mobility (μ) of carriers of Ag₂Cu₂O₃ thin films have been estimated from Hall measurements. Table (7) illustrates the main parameters estimated from Hall Effect measurements for Ag-Cu-O thin films deposited at room temperatures, and annealed at 200°C for half hour. We can notice from this table that all the samples have a positive Hall coefficient (p-type) similar results were obtained by P. Narayana Reddy et al. [17]. The conductivity decrease with increasing temperature of sintering for as deposited and annealed samples. The increase of the electrical resistivity with increasing sintering temperature may be due to the reduction in the crystallinity as shown in the XRD profile data, also as a result of decreasing the carrier concentration.

Table 7. Hall Effect measurements for Ag-Cu-O film with different thicknesses and different sintering temperature (200°C, 300°C and 600°C)

Thin films	Sintering temp.	thickness	ρ (1/ Ω cm)	n(cm ⁻³)	μ (cm ² /V.sec)	Type
As deposited	200°C	200nm	2.233×10^{-4}	8.401×10^{12}	1.659×10^2	P-Type
	300°C	200nm	2.399×10^{-5}	4.131×10^{12}	3.624×10^1	
	600°C	100nm	1.323×10^{-5}	2.372×10^{10}	3.482×10^3	
annealed	200°C	200nm	8.819	7.424×10^{14}	7.415×10^4	
	300°C	200nm	2.117×10^{-5}	2.785×10^{10}	4.746×10^3	
	600°C	100nm	2.884×10^{-5}	5.740×10^{11}	3.136×10^2	

Fig. (12) shows the sensitivity as a function of operation temperature at different sintering temperature (200°C, 300°C and 600°C) for Ag₂Cu₂O₃/n-Si films. The variation of the sensitivity with operation temperature increases as the temperature increases from room temperature to 100°C and decreases as the temperature increases from 100°C to 200°C which is showing a typical negative temperature coefficient of resistance (NTCR) due to the thermal excitation of the charge carriers in semiconductor. These thin films specimens are examined for chemical sensing using NO₂ at different operation temperature (R.T, 100°C and 200°C).

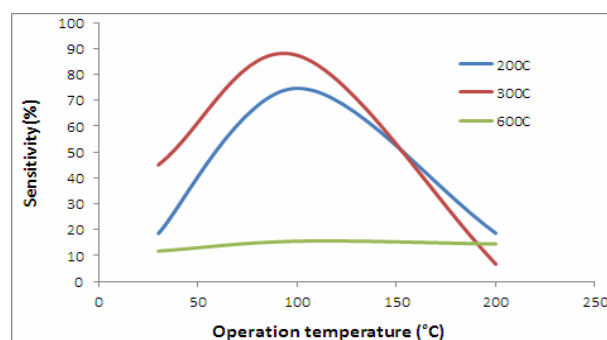


Fig.12. The variation of sensitivity with the operating temperature of $\text{Ag}_2\text{Cu}_2\text{O}_3$ deposited on silicon at different sintering temperature

Fig. (13) shows the relation between the response time and the Recovery time as a function of operation temperature with different sintering temperature (200°C , 300°C and 600°C) of the $\text{Ag}_2\text{Cu}_2\text{O}_3$ deposited on silicon. These figure shows that the increase of response \recovery time with increasing operation temperature from room temperature to 100°C then decrease with increasing operation temperature from 100°C to 200°C when sintering temperature 200°C and 300°C . At sintering temperature 600°C the response \recovery time decrease with increasing operation temperature from room temperature to 100°C then increase with increasing operation temperature from 100°C to 200°C .

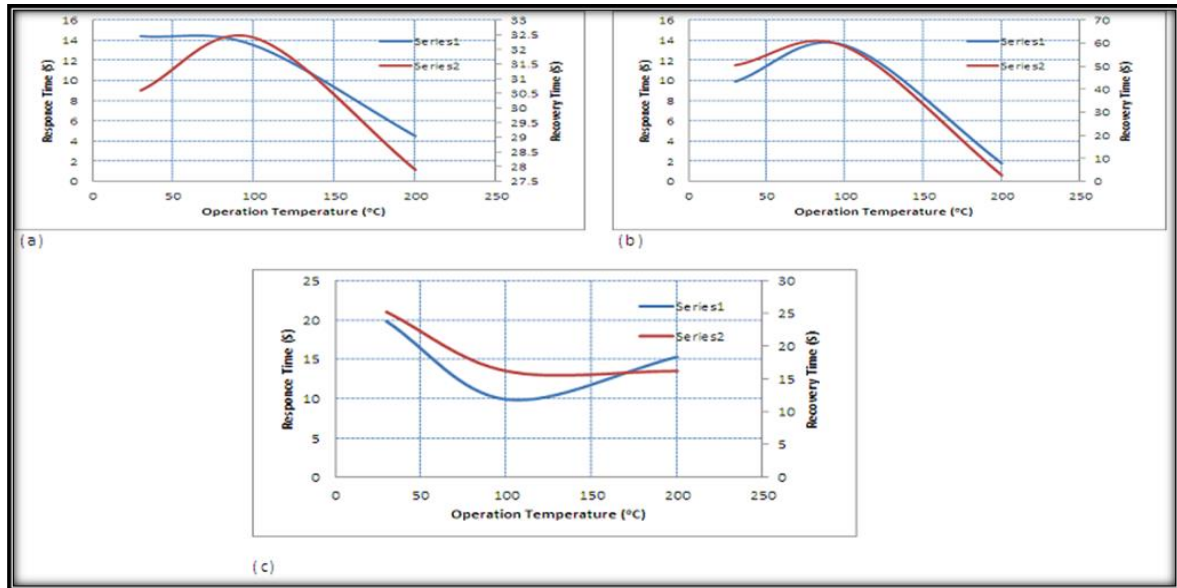


Fig.13. The variation of Response time and Recovery time with operating temperature of $\text{Ag}_2\text{Cu}_2\text{O}_3$ deposited on silicon at different sintering temperature (a) 200°C (b) 300°C and (c) 600°C

Table 8.The sensitivity, Response time and Recovery time

Sample	Sintering Temp.	Temp. ($^\circ\text{C}$)	S%	response time(sec)	recover time (sec)
$\text{Ag}_2\text{Cu}_2\text{O}_3/\text{n-Si}$	200°C	30	18.59	14.4	30.6
		100	74.64	13.5	32.4
		200	18.64	4.5	27.9
$\text{Ag}_2\text{Cu}_2\text{O}_3/\text{n-Si}$	300°C	30	45.03	9.9	50.4
		100	87.38	13.5	58.5
		200	6.72	1.8	2.7
$\text{Ag}_2\text{Cu}_2\text{O}_3/\text{n-Si}$	600°C	30	11.79	19.8	25.2
		100	15.60	9.9	16.2
		200	14.52	15.3	16.2

4. Conclusion

Ag-Cu-O films have been deposited on glass and Si substrate by pulsed laser deposition method. The effect of sintering temperature of powder, and the annealing temperature on the properties of Ag-Cu-O films were studied.

The powder sintered at 200°C have the best structure to obtain tetragonal Ag₂Cu₂O₃ phase as compared with others sintering temperature. Also the films which formed from this powder has a good structure with sharp peaks (high intensity) and the Ag₂Cu₂O₃ phase showed with good appearance. Surface topology by AFM analysis showed irregular shape of grains with big size and the increase of sintering temperature made the grains had regular shape with continuous granular morphology. The optical band gap decrease from 1.77eV to 1.45eV with increasing the sintering temperature to 300°C and then increase to 1.90eV when temperature of sintering equal to 600°C. The heat treatment of these films make the band gap narrow.

The electrical resistivity of these films increase with increasing the sintering temperature for as deposited and annealed.

The optimum sensitivity obtained for film prepared from powder which sintered at 300°C and at operating temperature equal to 100°C.

References

- [1] A. Sreedhar, M. H. Reddy, S. Uthanna, R. Martins, E. Elangovan, and J.F. Pierson *Acta Physica Polonica A* **120**(6), 37 (2011).
- [2] P. Gomez-Romero, E. M. Tejada-Rosales, M. Rosa Palacin, *Angewandte Chemie International Edition* **3**, 524 (1999).
- [3] J.F. Pierson, E. Rolin, C. Clément-Gendarme, C. Petitjean, D. Horwat, *Applied Surface Science* **254**, 6590 (2008).
- [4] C. Petitjean, D. Horwat, J.F. Pierson, *J. Phys. D: Appl. Phys.* **42**, 1 (2009).
- [5] C. D. May, J. T. Vaughney, *Electrochemistry Communications* **6**, 1075 (2004).
- [6] M. Hari Prasad Reddy, J. F. Pierson, S. Uthanna, *Cryst. Res. Technol.* **46**, 1329 (2011).
- [7] C. Petitjean, D. Horwat, J.F. Pierson, *Applied Surface Science* **255**, 7700 (2009).
- [8] D. Majumdar, H. D. Glicksman, T. T. Kodas *Powder Technology* **110**, 76 (2000).
- [9] K. Adelsberger, J. Curda, S. Vensky, M. Jansen, *Journal of Solid State Chemistry* **158**, 82 (2001).
- [10] E. M. Rosales, J.R. Arvajal, N. C. Pastor, P. Alemany, E. Ruiz, M. S. El-Fallah, S. Alvarez, P. Gómez-Romero, *Inorganic chemistry* **41**(25), 6604 (2002).
- [11] J. F. Pierson, D. Horwat, *Applied Surface Science* **253**, 7522 (2007).
- [12] C. C. Tseng, J. H. Hsieh, S. J. Liu, W. Wu, *Thin Solid Films* **518**, 1407 (2009).
- [13] D. Muñoz-Rojas, J. Oro, P. Gomez-Romero, J. Fraxedas, N. Casan-Pastor, *Electrochemistry Communications*, **4**, 684 (2002).
- [14] D. Muñoz-Rojas, J. Fraxedas, P. Gomez-Romero, N. Casan-Pastor, *Journal of Solid State Chemistry* **178**, 295 (2005).
- [15] J. Feng, B. Xiao, J. C. Chen, C. T. Zhou, Y. P. Du, R. Zhou, *Solid State Communications* **149**, 1569 (2009).
- [16] P. Narayana Reddy, A. Sreedhar, M. Hari Prasad Reddy, S. Uthanna, *ISRN Condensed Matter Physics* **2012**, 1 (2012).
- [17] D. Muñoz-Rojas, J. Fraxedas, P. Gomez-Romero, J. Oro, N. Casan-Pastor, *Crystal engineering* **5**, 459 (2002).